

Syntheses of Novel Protein Products (Milkglyde, Saliglyde, and Soyglyde) from Vegetable Epoxy Oils and Gliadin

Rogers E. Harry-O'kuru,^{*,†} Abdellatif Mohamed,[‡] Sherald H. Gordon,[‡] and James Xu[‡]

[†]Bio-Oils Research Unit and [‡]Plant Polymer Research Unit, National Center for Agricultural Utilization Research, Agricultural Research Service, U.S. Department of Agriculture, 1815 North University Street, Peoria, Illinois 61604, United States

ABSTRACT: The aqueous alcohol-soluble fraction of wheat gluten is gliadin. This component has been implicated as the causative principle in celiac disease, which is a physiological condition experienced by some infants and adults. The outcome of the ingestion of whole wheat products by susceptible individuals is malabsorption of nutrients resulting from loss of intestinal vili, the nutrient absorption regions of the digestive system. This leads to incessant diarrhea and weight loss in these individuals. Only recently has this health condition been properly recognized and accurately diagnosed in this country. The culprit gliadin is characterized by preponderant glutamine side-chain residues on the protein surface. Gliadin is commercially available as a wheat gluten extract, and in our search for new biobased and environmentally friendly products from renewable agricultural substrates, we have exploited the availability of the glutamine residues of gliadin as synthons to produce novel elastomeric nonfood products dubbed "milkglyde", "saliglyde", and soyglyde from milkweed, salicornia and soybean oils. The reaction is an amidolysis of the oxirane groups of derivatized milkweed, salicornia, and soybean oils under neat reaction conditions with the primary amide functionalities of glutamine to give the corresponding amidohydroxy gliadinyl triglycerides, respectively. The differential scanning calorimetry, thermogravimetric analyses, and rheological data from a study of these products indicate properties similar to those of synthetic rubber.

KEYWORDS: *oxirane triglycerides, milkweed oil, salicornia oil, soybean oil, gliadins, milkglyde, saliglyde, soyglyde, DSC, rheology, elastomer*

■ INTRODUCTION

The idea of functional degradable/biodegradable synthetic materials evolved from the observation of the polluting effects of nondegrading plastics in our ocean, lake, and land environments and the realization of the increasing need for more landfill space to accommodate these plastics. Functional and durable as current petroleum-based plastics are, their unintended consequences have convinced researchers to rethink solutions that would address the ecological problems being created by using such nondegrading plastics in the environment. Several approaches have been initiated over the years, which include the concept of photodegradation where a polymer such as polyethylene is synthesized incorporating functional groupings like carbonyls that could undergo photolysis in the environment during disposal. In principle, such modified polymers would breakdown photolytically via the Norrish type cleavage mechanisms at those carbonyl insertion points.^{1–4} Scission at such insertion points of the large polymers via the free radical depolymerization process induced by UV radiation was hoped to result at best in more manageable decomposition units. The resulting breakdown polymeric entities should finally result in smaller modular units that may be small enough for microorganisms in the environment to then colonize and metabolize, thus initiating a solution to the huge pollution problems. A completely novel approach was the development polyesters and polyamides that are truly biodegradable. Such polymers are the polycaprolactams/polycaprolactones,⁵ polyhydroxybutyrate (PHBs), polyhydroxybutyrate-co-valerates (PHBVs),⁶ and polylactides, etc., with specialized uses.^{7–13} Another unique initiative was that of

incorporating naturally biodegradable substrates like starch and cellulose into traditional polyethylene and polypropylene plastics during manufacture in the hope that the carbohydrate component would form a springboard from which microbial colonization and degradation of the whole plastic would occur after its useful lifetime.^{14,15} In a newer generation of plastics, glycidyl monomers such as bisphenol A diglycidyl ether or bisphenol A propoxylate diglycidyl ethers on one hand and alkyldiamine monomers have been utilized to synthesize aminohydroxy polymers that could biodegrade in the environment after disposal. However, such BPA polymeric products, important as they may be, provide us no answers to the improvement of the quality of our already polluted and degraded environment since the breakdown products of the latter add to rather than ameliorate the problem. As part of a continuing effort to a solution to this nagging problem, we here describe a reaction process utilizing gliadin and modified new crop oils, two completely renewable materials, to generate novel elastomeric protein derivatives at moderate temperatures that could be used as stable environmentally friendly materials within and after their application lifetimes. Gliadin has been implicated as the causative agent in celiac disease, a condition that results in malabsorption of nutrients and therefore weight loss in susceptible infants and adults.^{16–21} However, as a reagent in this nonfood application, gliadin holds much promise

Received: August 12, 2011

Revised: January 12, 2012

Accepted: January 17, 2012

Published: January 17, 2012

for the wheat grower as well as the processor and end user as a biomaterial feedstock for amidohydroxy gliadinyl triglycerides and other products that exhibit novel elastomeric properties.

MATERIALS AND METHODS

Materials. Milkweed (*Asclepias syriaca* L.) oil was obtained from Natural Fibers Corp. (Ogallala, NE), and salicornia (*Salicornia bigelovii* Torr) oil was from Seaphire (Phoenix, AZ). Hydrogen peroxide (50%), formic acid (99%), and anhydrous ZnCl_2 were purchased from ACROS Organics (Chicago, IL), and gliadin was obtained from Midwest Grain Products, Inc. (Atchison, KS).

Instrumentation. *Fourier Transform Infrared (FT-IR) Spectrometry.* FT-IR spectra were measured on an Arid Zone FT-IR spectrometer (ABB Bomem-Series, Houston, TX) equipped with a DTGS detector. Dried solid test samples were pulverized with KBr (1/300 mg) and pressed at 24000 psi to generate transparent discs for FT-IR analysis. Liquid derivatives were pressed between two NaCl discs (25 mm \times 5 mm) to give thin transparent oil films for analysis by FT-IR spectrometry. Absorbance spectra were acquired at 4 cm^{-1} resolution and signal-averaged over 32 scans. Interferograms were Fourier transformed using cosine apodization for optimum linear response. Spectra were baseline corrected, adjusted for mass differences, and normalized to the methylene peak at 2927 cm^{-1} .

NMR Spectroscopy. The ^1H and ^{13}C NMR spectra were recorded on a Bruker ARX-500 spectrometer with a 5 mm dual proton/carbon probe (Bruker Spectrospin, Billerica, MA); the internal standard was tetramethylsilane.

Differential Scanning Calorimetry (DSC). DSC analysis was performed on a Q2000 MDSC (TA Instruments, New Castle, DE).

Rheometry. A strain-controlled Rheometric ARES rheometer (TA Instruments, Inc.) was used to perform the rheology studies.²⁵ An 8 mm diameter plate-plate geometry was adopted. The temperature was controlled at 25 ± 0.1 $^\circ\text{C}$ by a water circulation system.

Methods. *Synthesis of Milkweed Epoxy Triglyceride.* In a typical process, 582.0 g of reprocessed milkweed oil (673.76 mmol, iodine value, IV = 111.4) was placed in a 1 L three-necked jacketed flask equipped with a mechanical stirrer and heated to 45.5 $^\circ\text{C}$. Formic acid (96%, 39.7 g, 0.3 equiv/mol of C=C) was added, and the mixture was stirred to homogeneity. Hydrogen peroxide (50%, 320 mL, 5.65 mol) was then added slowly (i.e., dropwise). At the end of hydrogen peroxide addition, the temperature was raised to 70 $^\circ\text{C}$, and vigorous stirring was continued for 7 h when a sample of the reaction mixture showed complete absence of the vinylic protons of the starting material. The heat source was then removed, and the reaction mixture was allowed to cool to near room temperature and transferred to a separatory funnel with ethyl acetate as diluent. The material was washed with saturated NaCl (300 mL \times 4) followed by saturated Na_2CO_3 (40 mL) in more NaCl solution. The washes were discarded. When pH 7.5 was reached, the organic phase was then washed with deionized water. The organic layer was separated from a turbid aqueous phase, dried over Na_2SO_4 , and concentrated at 60 $^\circ\text{C}$ in vacuo to remove the solvent. The yield of the epoxy triglyceride was 558.4 g; the kinematic viscosities measured were as follows: $\eta_{40^\circ\text{C}}$ = 164.4 cSt and $\eta_{100^\circ\text{C}}$ = 19.22 cSt, that is, a viscosity index of 133; PV = 9.4, and IV = 1.79. Specific rotation $[\alpha]_{\text{D}}^{20}$ = +0.17 $^\circ$. FT-IR (film on NaCl discs) cm^{-1} : 3471 w, 2927 vs, 2856 vs, 1743 vs, 1560 w, 1463 s, 1375 s, 1242 s, 1162 s, 1105 s, 1048 s, 845–824 d(m), 726 w-m. ^1H NMR (main fraction in CDCl_3) δ (ppm): 5.25 m (residual vinylic), 4.29 dd (J = 4.3, 11.9 Hz, 2H), 4.14 dd (J = 5.9, 11.9 Hz, 2H), 3.1 m (2H), 2.96 m (2H), 2.89 m (2H), 2.3 m (6H), 1.75–1.25 m (72H), 0.87 m (9H). ^{13}C (CDCl_3) δ (ppm): 173.1, 172.7 (C=O); 68.87 (–CHO– glyceride backbone); 62.02 (–CH₂O– glyceride backbone); 57.10, 57.05, 56.91, 56.85, 56.63, 56.55, 54.25, 54.09 (–C–O–C– epoxide); 34.06, 33.90 (α -CH₂–); 31.79,

31.61 (C11 of linoleyl moieties); 29.63, 29.47, 29.28, 29.23, 29.15, 29.12, 28.92, 28.88 (–CH₂– contiguous to hydroxylated carbons); 27.83, 27.77, 27.75, 27.16, 26.88, 26.55, 26.52, 26.08, 24.73 (–CH₂–); 22.51 (–CH₂– next to terminal –CH₃); 13.93 (terminal –CH₃).

Synthesis of Milkglyde: Amidohydroxy Gliadinyl Glyceride of Milkweed Epoxide. In a semiscaled up reaction, milkweed epoxide (250.0 g, 262 mmol) was placed in a dry 1.0 L jacketed and fully baffled reactor into which were added dry powdered gliadin (110.0 g) and anhydrous ZnCl_2 (5.7 g). The reactor was equipped with an overhead stirrer and a heat regulator bath. The bath was connected and started, and the temperature was set to 70 $^\circ\text{C}$. Meanwhile, the reactor contents were gently purged with N_2 for 30 min after which the stirrer was started. Stirring was continued and occasionally adjusted until completion of reaction when the product solidifies into a rigid state. The heat source was turned off, the system was allowed to cool to room temperature, and the product was reclaimed from the reactor by pulling it out. It had a slight tack and sheen, which were removed with a quick acetone wash and drying in air to give 347.7 g (96.6%) of an elastic solid. Its FT-IR spectrum on KBr disk is ν_{KBr} cm^{-1} : 3426 s (–N–H, O–H stretch), 2927vs (–CH₂– asym stretch), 2855 s (–CH₂–, –CH₃ sym stretch), 1743 s (ester C=O), 1658 s (amide I), 1534 m (amide II), 1458 (–CH₂– deform), 1384 s (–CH₃ deform), 1244 (–OC–C– ester stretch), 1168 (–CHO–), 1095 (–C–CHO–), 723 (–CH₂– wag).

Synthesis of Salicornia Epoxy Triglyceride. In a dry 1000 mL three-necked, round-bottomed jacketed flask equipped with an overhead stirrer and heated to 40 $^\circ\text{C}$, salicornia oil (475.5 g, 583.65 mmol, iodine value = 132.8) and 99% formic acid (49.56 g, 40.6 mL) were placed. The reaction mixture was vigorously stirred to homogeneity, and hydrogen peroxide (50%, 274.87 g, 4.0416 mol, 232.9 mL) was added slowly. At the end of peroxide addition, the reaction temperature was raised to 70 $^\circ\text{C}$, while vigorous stirring was continued for 5 h when the FT-IR spectrum of a reaction sample showed complete reaction. The heat source was turned off, and the reaction was allowed to cool to room temperature. The contents of the reaction vessel were diluted with ethyl acetate (300 mL) and transferred into a separatory funnel. The separated aqueous layer was removed, and the organic phase was washed sequentially with brine (2 \times 400 mL) followed with saturated Na_2CO_3 solution (50 mL) in additional saturated NaCl solution. The organic layer was then dried over Na_2SO_4 and concentrated under reduced pressure to give a colorless slightly viscous liquid (548.9 g). An overnight drying of the product at the pump yielded 512.9 g (98.9%) of the polyepoxy triglyceride. A transparent film of this product on NaCl discs showed the following FT-IR spectral bands, ν_{NaCl} cm^{-1} : 2927 vs (–CH₂– asym stretch) and 2856 s (–CH₃, –CH₂– sym), 1756 vs (O=C< ester), 1463 m-s (–CH₂– def), 1377 m (–CH₃ def), 1241 m-s (O=C–C), 1161 s (–CHO–), 1104 (–CHO–), 1048 (–CH₂O–), 844–825 d (–C–O–C– asym. epoxide stretch), 726 (–CH₂– wag). In contrast, the native oil gave IR bands that included 3019 cm^{-1} w-m (H–C=C–) and 1654 vw (C=C breathing mode of the olefin). ^1H NMR (CDCl_3) δ (ppm): 5.26 bs (1H), 4.31 d (J = 11 Hz, 1H), 4.13 m (4H), 3.09 d (J = 23 Hz, 4H), 2.93 d (J = 38.2 Hz, 4H), 2.32 s (6H), 2.04 d (J = 3.6 Hz, 2H), 1.8–1.2 m (69H), 0.90 bs (9H). ^{13}C NMR (CDCl_3) δ (ppm): 173.14, 172.74 (C=O); 68.90 (CHO glyceryl); 62.08, 60.34 (–CH₂O– glyceryl); 57.17, 57.11, 56.98, 56.91, 56.70, 56.62, 54.31, 54.15 (epoxy carbons); 34.12 (C-2), 33.95 (C-2), 31.65 (C-16), 29.67(C-16), 29.64 (C-5), 29.52 (C-5), 29.33 (C-14), 29.29 (C-14), 29.25 (C-7), 29.16 (C-7), 28.97 (C-8), 27.89, 27.87, 27.82, 27.80, 27.21, 26.92, 26.59, 26.55, 26.44, 26.23, 26.12, 24.79 (C-3), 24.76 (C-3), 22.55 (C-17); 14.18 (C-18), 13.96 (C-18) ppm.

Synthesis of Saliglyde: Gliadinyl Amidohydroxy Triglyceride of Salicornia Epoxide. In a typical reaction, salicornia epoxide (250.0 g, 261.6 mmol) was placed in a dry 1.0 L jacketed and baffled three-necked reactor equipped with an overhead stirrer. Dry powdered gliadin (100.0 g) together with anhydrous ZnCl_2 (4.6 g) were added. The heat regulator was started with a setting of 80 $^\circ\text{C}$, and the reactor contents were gently purged with N_2 (30 min). Thereafter, the stirrer was started, and the reaction mixture was stirred to homogeneity.

Stirring was continued, and the reaction was monitored in 5 h intervals by FT-IR until the epoxy C—O—C band at 845–824 cm^{-1} disappeared or when the stirrer stopped moving. The product was allowed to cool to near room temperature so it could be pulled out of the reactor and rinsed for 2 min with acetone and allowed to air-dry in the hood; the yield was 355 g, >97%, an elastic solid. FT-IR spectrum ν_{KBr} cm^{-1} : 3432 s (—N—H, —O—H stretch), 2928 vs (—CH₂— asym. stretch), 2856 s (—CH₃, —CH₂— sym. stretch), 1743 vs (>C=O ester), 1655 s (amide I), 1533 (amide II), 1465 (—CH₂— def), 1384 s (—CH₃ def), 1272 (O=C—C), 1166 (O—C—C—), 1075 (—CHO), 723 (—CH₂— wag).

Synthesis of Epoxy Soybean Triglyceride. In a dry 1000 mL three-necked jacketed reactor equipped with an overhead stirrer and an addition funnel and heated to 40 °C was added soybean oil (432.8 g, 0.494 mol). The oil was stirred vigorously, and formic acid (99%, 34.12 g, 0.3 equiv) was added in one portion. This was followed by dropwise addition of 50% H₂O₂ (336 g, 9.88 mol). At the end of H₂O₂ addition, the reaction temperature was raised to 70 °C, and the reaction progress was monitored at 30 min intervals by FT-IR spectrometry. At the end of 2 h, an FT-IR spectrum of a reaction sample showed complete disappearance of the 3010 cm^{-1} band of the starting olefin in the reaction product, the heat was turned off, and the system was allowed to cool to room temperature as stirring continued. The product mixture was diluted with ethyl acetate and poured into a stirring solution of saturated NaCl/Na₂CO₃. After effervescence had subsided, the organic phase was separated, and the aqueous layer was extracted with more EtAc (200 mL \times 3). The combined organic phase was dried over Na₂SO₄ and concentrated under reduced pressure at 57 °C to give a quantitative yield of 492.7 g. FT-IR spectrum (film on NaCl discs) ν cm^{-1} : 2927 vs, 2855 s, 1741 vs, 1461 m-s, 1381 m, 1241 m, 1161 s, 1101 m, 1021 w, 844–824 d, 722 m.

Synthesis of Amidohydroxy Gliadinyl Triglyceride (Soyglyde). To 250 g, 262 mmol of epoxysoybean oil in a 1 L three-necked, jacketed reaction kettle at 70 °C was added powdered gliadin (110.0 g), with 5.0 g of anhydrous ZnCl₂. The setup was purged with N₂ for 15 min before the mixture was vigorously stirred. The reaction was monitored every 3 h by FT-IR spectroscopy for the disappearance of the stretching doublet of the epoxy moiety at 824–840 cm^{-1} . Because this band diminished very slowly, two more aliquots of gliadin (25.0 g and then 30.0 g) were added successively to the reaction until the epoxy bands were consumed or nearly so. Thus, 262 mmol of epoxysoybean oil required 165.0 g of gliadin and 10.0 g of ZnCl₂ for complete reaction to produce 387.8 g of the soy oil amidohydroxy gliadinyl triglyceride or soyglyde. Its FT-IR ν_{KBr} cm^{-1} : 3411 (N—H, OH), 2956 sh (CH₃ asym str.), 2930 vs (CH₂ sym. str), 2855 s (CH₂ asym str.), 1743 vs (C=O ester), 1657 vs (amide I, HN—C=O), 1535 m (amide II), 1454 m (CH₂ deform), 1383 s (CH₃ deform), 1239 m (OC=O—C), 1160 s (CHO stretch), 1060 m-s (NH, HCOH), 722 w (CH₂ wag).

Thermal Analysis of Saliglyde (Amidohydroxygliadinyl Triglyceride) and Milkglyde. Thermogravimetric analysis (TGA) was performed as follows: a sample (32–35 mg) was placed on an open platinum TGA pan and loaded on the TGA. The sample was heated in a nitrogen atmosphere at 10 °C/min to 800 °C. The derivative TGA of the sample showed initial degradation between 150 and 200 °C, with the main degradation peaking at 399.6 °C and a smaller peak at 449.7 °C. The compound showed 14% undegraded residue at 800 °C (Figure 6).

Differential Scanning Calorimetry. The sample (23–25 mg) was sealed hermetically in a stainless steel DSC pan and tested using modulated DSC; heating rate 5 \pm 1 °C/min and thus to view the reversing and nonreversing heat flow results separately. The initial sample was cooled to –88 °C at a rate of 5 °C/min and subsequently heated at the same rate (with modulation) to 150 °C. This method was repeated for a second cycle. To eliminate the thermal history of the material, a second sample was heated first from room temperature to 150 °C, then cooled to –88 °C, and heated again (all at 5 °C/min). From the TGA data, it was established that the compound started degrading around 200 °C instead of 150 °C. So, instead of 150 °C, a new sample was heated to 200 °C right around the start of

degradation. The material exhibited an exothermic transition at 168.5 °C.

Rheological Measurements. Linear viscoelastic measurements were conducted for the composites. To ensure that all of the measurements for the materials were made within the linear viscoelastic range, a strain-sweep experiment was conducted initially. An applied shear strain valued in the linear range was adopted for the other viscoelastic property measurements for the same material; new samples were used for each experiment. A 0.1% shear strain was used for the measurements of all three composites. Linear viscoelasticity indicates that the measured parameters are independent of applied shear strain. Small-amplitude oscillatory shear experiments strain were conducted over a frequency (ω) range of 0.1–500 rad/s, yielding the storage or elastic (G') moduli and loss (G'') moduli. The storage modulus represents the nondissipative component of mechanical properties. The elastic or “rubberlike” behavior is suggested if the G' spectrum is independent of frequency and greater than the loss modulus over a certain range of frequency. The loss modulus represents the dissipative component of the mechanical properties and is characteristic of viscous flow. The phase shift or phase angle (δ) is defined by $\delta = \tan^{-1}(G''/G')$ and indicates whether a material is solid with perfect elasticity ($\delta = 0$), or fluid with pure viscosity ($\delta = 90^\circ$), or something in between. Stress relaxation measurements were also performed in the linear viscoelastic range. Stress relaxation experiments measured the stress relaxation with the time after the material is subject to a step increase in shear strain.

RESULTS AND DISCUSSION

Realization of the Norrish type mechanisms in mitigating marine and other aquatic pollution from industrial plastics has not been achieved. This may be either because the loading of the requisite UV active components is not adequate in the plastic or that the process takes too long to manifest the desired result in the environment. In pursuit of such materials, chemists have ingeniously explored a horizon of ideas from incorporating different functional groupings like >C=O into nondegradable but readily available paraffinic substances in the manufacture of polyethylenes, polypropylenes, etc. Polylactides, PHBs, and PHBVs were also a result of this effort. The former (>C=O) polymers were hoped with time to photolytically break down via the Norrish type cleavage mechanisms at the carbonyl insertion points into more manageable decomposition units. The use of renewable biomaterials to construct such a biodegradable milieu is more novel starting with PHB, PHVB, and polylactides, which although truly biodegradable had specialized applications. Pursuant to a similar objective, we have utilized the preponderant pendant glutamine side-chain residues of gliadin, which would be accessible on the protein surface to the oxirane units of vegetable oils as synthons to construct new biobased products by amidolysis of the glycidyl functional groups of derivatized milkweed, salicornia, and soybean oils. Gliadin is a rich source of glutamine side-chain residues as is apparent from the proposed sequence shown in Figure 1. No other known protein is like it. These residues in whole wheat protein have been referred to as the causative agents in celiac disease, a debilitating condition in susceptible infants and adult persons that is symptomatic of intestinal malabsorption of nutrients because of loss of absorptive intestinal surfaces (vili), thus producing weight loss and chronic diarrhea.^{14–18} The reaction of gliadin with the oxirane of milkweed, salicornia, and soybean oils on the other hand is an addition reaction, more precisely an amidolysis of the oxirane units resulting in the gliadinyl amidohydroxy triglycerides. Because the primary amide (O=C—NH₂) functional group is not an avid nucleophile, this reaction is nudged on by the

MKTFLLALLAIVATTAVRVPVLPQLPQNPSQQPQ
 EQVPLVQQQQLGQQPFPQPYPQPFPSPQPYLQLQ
 PFLQPQLPYSQPQFRPQQPYPQPQYSQPQPISQQQ
 QQQQQQQQQQQQQIIQILQQLIPCMDVVLQQHNV
 HGKSQVLQQSTYQLLQELCCQHLWQIPEQSQCAIHNVVH
 AILHQQQKQQQPSQVFSFQQPLQQYPLGQGSFRPSQQ
 NPQAQGSVQPQLPQFEEIRNLARK

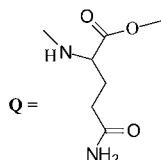


Figure 1. Segment of the proposed structure sequence of gliadin. Georges-Louis Friedli's Ph.D. Thesis, University of Surrey, England; also in refs 16 and 18.

presence of the Lewis acid, $ZnCl_2$, as the catalyst (Figure 4). The $ZnCl_2$ activates the oxirane carbons toward amidolysis by coordination to the epoxy oxygen. This is attested to by the characteristically narrow IR spectral absorption band (3426 cm^{-1}) of the product in contrast to the broad primary amide bands of the starting protein. The intensity of the above band is a consequence of overlap of the generated secondary alcohol (O–H) moieties with the secondary amides (–N–H) stretching modes. Also, the spectral region between 1800 and 1500 cm^{-1} is marked by the ester carbonyl absorption of the triglyceride component (1743 cm^{-1}) and the amide I' and amide II' modes of the protein and the new secondary amide components at 1658 and 1534 cm^{-1} , respectively, as observed in Figures 2 and 3. The other glaring feature in the spectrum of

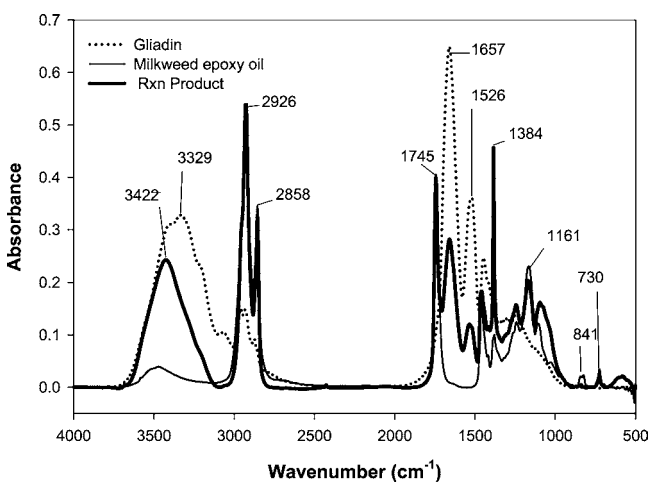


Figure 2. Overlaid FT-IR spectra of gliadin, milkweed epoxide, and their reaction product, amidohydroxy gliadyl triglyceride (milkglyde).

each product is the disappearance of the doublet at $845\text{--}825\text{ cm}^{-1}$, a band characteristic of the oxirane $\text{C}=\text{O}-\text{C}$ asymmetric stretching mode of epoxy ring (Figures 2 and 3).^{23,24} Because milkglyde, saliglyde, and soyglyde are highly insoluble in all known NMR solvents, this technique has not been available for additional chemical characterization purposes. The physical nature of the products resulting from stoichiometric ratios of reaction of the epoxide with gliadin is an elastic solid with a small amount of tack so that the product is recovered from the reaction vessel by being physically pulled out with little or no loss of product. When desired, however, a

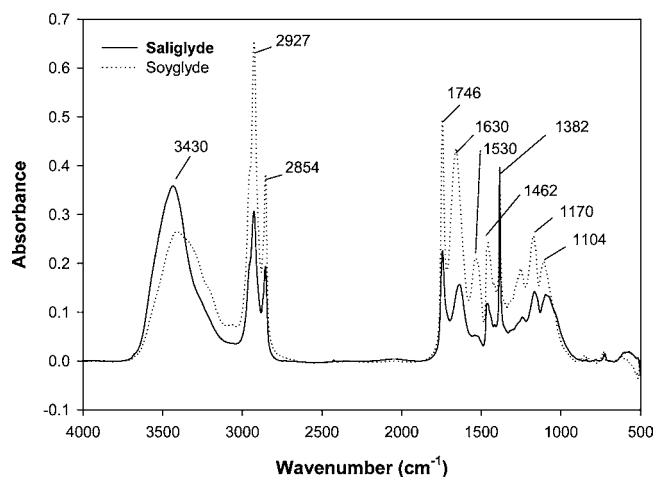


Figure 3. Overlaid FT-IR spectra of amidohydroxy gliadyl triglyceride (saliglyde) and soyglyde.

stable, pourable intermediate product of this reaction that could be easily used as a biomaterial coating medium could be derived in the case of Milkweed oxirane by treating say 250.0 g of the oxirane, for instance, with only 72% of the amount of gliadin needed for the stoichiometric reaction under the same reaction conditions. Under this condition, the FT-IR spectrum of the intermediate does indicate the presence of some primary amide $\text{O}=\text{C}-\text{NH}_2$ modes as in the starting material (3400 to 3100 cm^{-1}) as well as some oxirane absorption band of the starting oil ($822\text{--}840\text{ cm}^{-1}$), respectively. This could also be applicable with salicornia and soybean epoxides at lower gliadin ratios. Otherwise, the complete reaction product is generated when stoichiometric rates of reagents are employed as seen in the saliglyde FT-IR spectrum (Figure 3).

The DSC thermograms of saliglyde, milkglyde, and soyglyde exhibited an exothermic transition at $168.5\text{ }^\circ\text{C}$ (Figure 5). This transition showed that before degrading the compound did go through aggregation. This aggregation does not amount to degradation because this sample showed a glass transition when it was cooled from 200 to $-80\text{ }^\circ\text{C}$. Not only that, the sample profile was superimposable on that of the earlier sample that had been heated to $150\text{ }^\circ\text{C}$. The DSC thermograms of saliglyde and milkglyde showed two glass transitions between -50 and $0\text{ }^\circ\text{C}$, where the peaks of the transitions were at -37 and $-16.2\text{ }^\circ\text{C}$ for saliglyde and -37.9 and $16.6\text{ }^\circ\text{C}$ for milkglyde (Figure 5 and also in Table 1). When samples of the material were dried using TGA and dynamic vapor sorption (DVS), similar results were obtained. The TGA-dried sample (dried at $110\text{ }^\circ\text{C}$ for 3 h under nitrogen) showed a very similar profile, whereas the DVS-dried sample (dried at $85\text{ }^\circ\text{C}$ and 0% humidity for 2 days) showed a $2\text{--}3\text{ }^\circ\text{C}$ shift in the middle temperature range of the two glass transitions (from -37 and $-16.2\text{ }^\circ\text{C}$ to -23.8 to $-5.5\text{ }^\circ\text{C}$), and even though the glass transition temperature had shifted, the ΔC_p values were similar.

The derivative of the TGA spectrum of saliglyde sample in nitrogen showed initial degradation between 150 and $200\text{ }^\circ\text{C}$, with the main degradation peaking at $399.6\text{ }^\circ\text{C}$ and a smaller peak at $449.7\text{ }^\circ\text{C}$ (Figure 6). Saliglyde in air exhibited three degradation peaks at 336.2 , 398.9 , and $595.1\text{ }^\circ\text{C}$ (Figure 6). It is clear that the degradation mechanism in air is different from that in nitrogen due to the reactivity of oxygen. Milkglyde in nitrogen showed one main degradation peak at $394.0\text{ }^\circ\text{C}$ and two shoulders at 325.5 and $449.5\text{ }^\circ\text{C}$ (Figure 6), while in air, it

Formation of Amidohydroxygliadinyl triglycerides

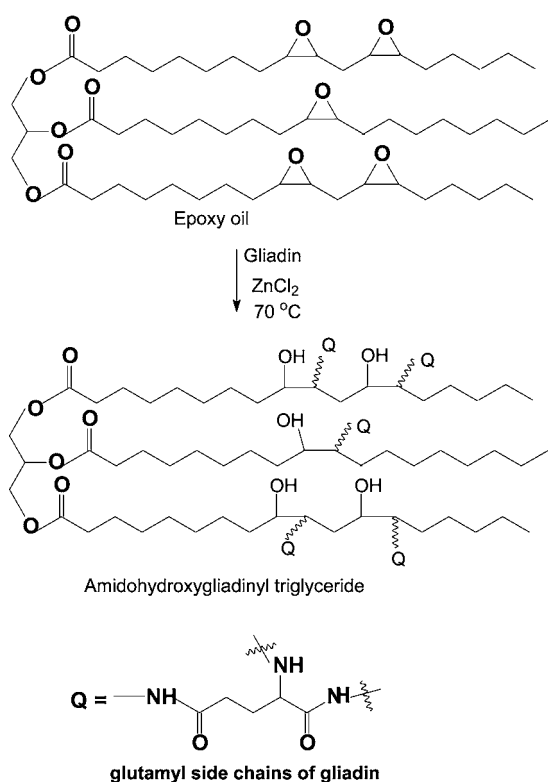


Figure 4. Formation of amidohydroxy gliadinyl triglycerides.

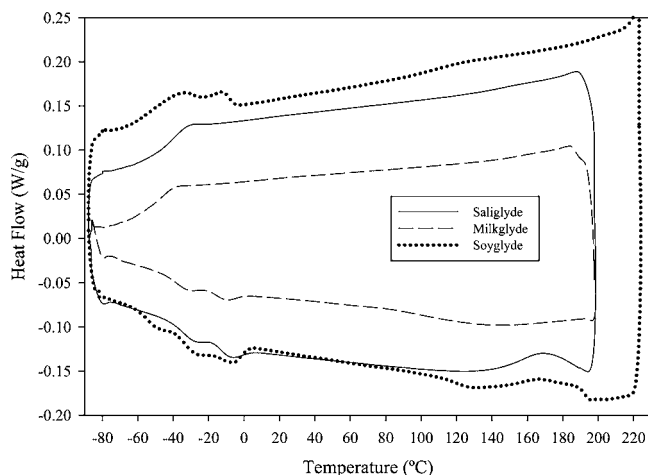


Figure 5. DSC thermograms of saliglyde, milkglyde, and soyglyde.

Table 1. Temperatures of the Two Glass Transitions Observed in Saliglyde, Milkglyde and Soyglyde Sample DSC Thermogram

transition	°C			ΔC_p (J/g °C)
	onset <i>T</i>	middle <i>T</i>	end <i>T</i>	
saliglyde Tg #1	-42.8	-37.0	-31.1	0.276
saliglyde Tg #2	-18.7	-16.2	-13.6	0.133
milkglyde Tg #1	-43.8	-37.9	-32.1	0.213
milkglyde Tg #2	-19.4	-16.6	-13.8	0.0854
soyglyde #1	-56.9	-51.9	-47.2	0.376
soyglyde #2	118.9	127.0	135.1	0.239

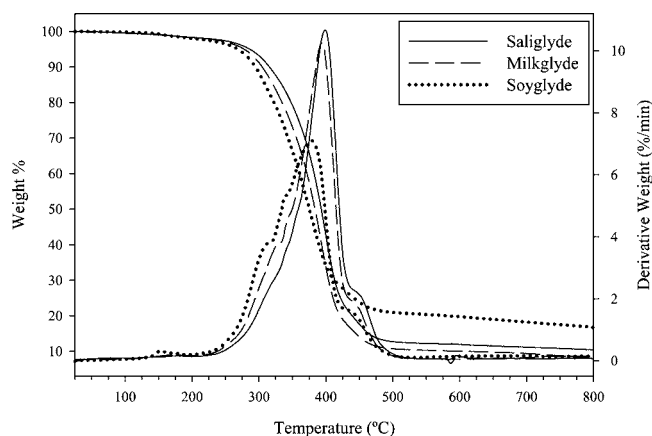


Figure 6. TGA of saliglyde, milkglyde, and soyglyde in nitrogen.

exhibited degradation peaks at 267.9, 323.3, 388.7, 398.9, and 543.2 °C with 47% of the degradation occurring at 398.9 °C. The compounds showed 14% undegraded residue at 800 °C in nitrogen, while in air 5.3% remained undegraded (Figure 6).

For soyglyde, the same sample size (23–25 mg) was hermetically sealed in a stainless steel DSC pan. The sample was run using modulated DSC (± 1 °C every 60 s) to view the reversing and nonreversing heat flow results separately. The initial sample was cooled to -88 °C at a rate of 5 °C/min and then heated at the same rate (with modulation) to 150 °C. This method was repeated for a second cycle; however, there was no change in the results. A second sample was heated first to 150 °C from room temperature, then cooled to -88 °C, and heated again (all at 5 °C/min). Again, the results remained the same. This second sample was also heated to 200 °C on the second cycle to see if there were any differences. The only difference after heating to 200 °C was a slight exothermic peak, which is most likely the beginning stages of decomposition. (After the run, the pan was opened, and the sample showed some browning, which corresponds to degradation.)

The DSC results showed a possible glass transition between -50 and 0 °C, with a possible two-part transition. The peaks of the transition were at -27 and -7.8 °C. Analyzed as two separate glass transitions, the results are shown in Table 1. It is clear from the table that the second glass transition of soyglyde was observed above zero at 127.0 °C, which is different from saliglyde and milkglyde, where both glass transitions appeared below zero.

The effect of drying method on the thermal properties of the composite was done by heat drying and low relative humidity. Samples of soyglyde were also dried using TGA and DVS, with similar results. The TGA-dried sample (dried at 110 °C for 3 h in nitrogen) showed a very similar DSC profile, while the DVS-dried sample (dried at 85 °C and 0% humidity for 2 days) showed a 2–3 °C shift in the peak temperature of the two peaks (from -27 and -7.8 °C to -23.8 and -5.5 °C). The glass transition temperatures also shifted; however, the ΔC_p values were similar.

Thermogravimetric Analysis of Soyglyde. The TGA was performed as follows: a sample (32–35 mg) was placed on an open platinum TGA pan and loaded on the TGA. The sample was heated in nitrogen or air atmosphere at 10 °C/min to 800 °C. The TGA derivative of soyglyde showed a slight initial degradation between 150 and 200 °C, with the main degradation peaking at 399 °C (there is also a shoulder around 450 °C). The derivative of the TGA of milkglyde also showed a

slight initial degradation; however, it began degrading sooner than soyglyde, with the main degradation peaking at 394 °C. The samples run in an air atmosphere showed very similar degradation profiles (Figure 7); on the derivative TGA, the

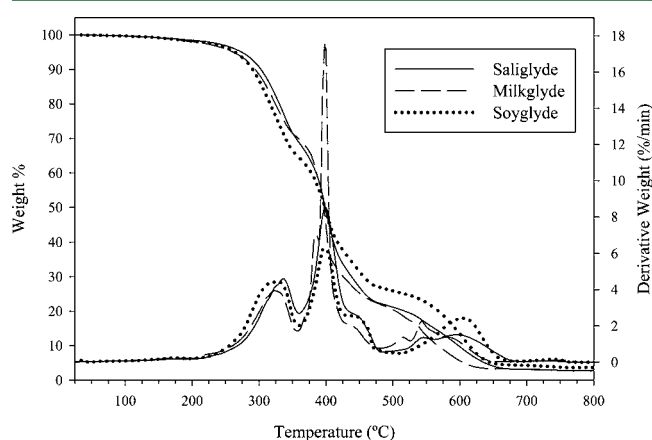


Figure 7. TGA of saliglyde, milkglyde, and soyglyde in air.

saliglyde showed degradation peaks at 336, 398, and 595 °C, while the milkglyde showed peaks at 323, 398, and 543 °C. Soyglyde showed a similar TGA profile as the milkglyde.

Rheometry. All three composites of saliglyde, milkglyde, and soyglyde exhibited viscoelastic solid behavior. The storage moduli (G') were greater than the loss moduli (G'') at all measured frequencies (Figure 8). Figure 8 displays the linear

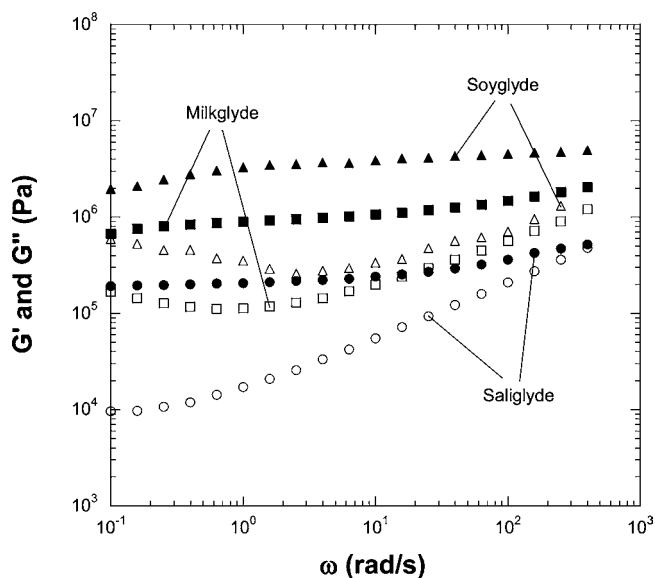


Figure 8. Linear dynamic viscoelastic properties of the composites saliglyde, milkglyde, and soyglyde at 25 °C with 0.1% strain. Filled symbols, elastic or storage modulus (G'); opened symbols, loss modulus (G''). Composite saliglyde (●, ○), composite milkglyde (■, □), and composite soyglyde (▲, △).

viscoelastic properties of the composites at 25 °C.²⁵ Among the three composites, soyglyde showed the strongest viscoelastic solid properties, while the saliglyde exhibited the weakest (Figure 8). The storage moduli (G') for all three composites were almost independent of the frequency, and the curve had a plateau over the three frequency decades, which was similar to that for rubber.²⁶ Their loss moduli (G'') curves were lower

than those of G' at all measured frequencies but were relatively more frequency-dependent, especially for the composite saliglyde (Figure 8). The elastic or storage moduli (G') at 1 rad/s were about 3.3×10^6 , 9.0×10^5 , and 2.1×10^5 for the soyglyde, milkglyde, and saliglyde, respectively. The phase shifts (δ) were in the range of 4.2–22.7°, 7.2–30.5°, and 2.9–42.8° for the soyglyde, milkglyde, and saliglyde, respectively. The shape of the G' curve for the milkglyde composite was also very similar to that of rubber.²⁶ In the preparation of soyglyde, the soyepoxide required a greater amount of gliadin reagent for reaction completion than was needed in epoxy milkweed reaction. This reflects the higher level of unsaturation and therefore a greater cross-linker capacity in soybean oil than its milkweed counterpart. Thus, soyglyde exhibited the strongest viscoelastic solid behavior among the three composites, and it is also reasonable that milkglyde showed stronger viscoelastic properties than saliglyde since milkweed oil had more cross-linking capacity than salicornia oil. Thus, the cross-linking capacity controlled the rheological properties of the three composites. For reference, a lightly cross-linked polymer, Hevea rubber, exhibits elastic modulus about 7×10^5 Pa at 25 °C,²⁶ and some synthetic elastomers, such as styrene-butadiene rubber and chloroprene rubber, display elastic moduli in the range of 1×10^6 to 3×10^6 Pa.²⁷ Therefore, the elasticity of all three composites was very close to those for some natural and synthetic rubbers. Stress relaxation experiments for the composite were also conducted (Figure 9). The

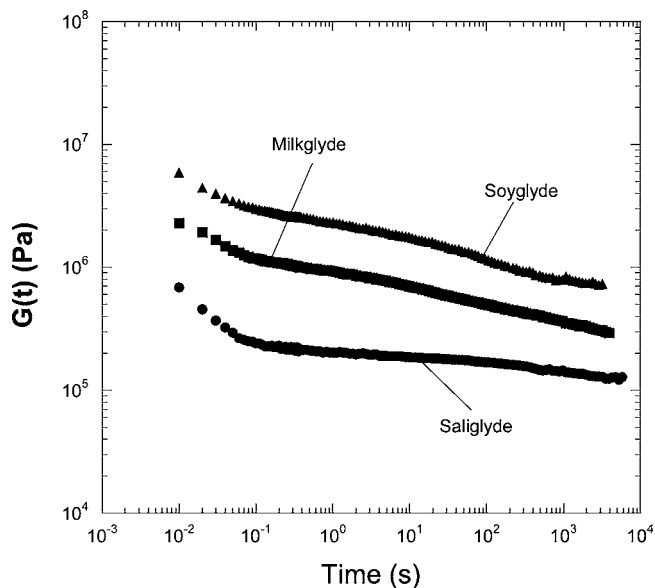


Figure 9. Stress relaxation measurement of the composites saliglyde, milkglyde, and soyglyde at 25 °C. The initial step strain was 0.1%. Composite saliglyde (●), composite milkglyde (■), and composite soyglyde (▲).

relaxation spectrum indicated that all three composites only relaxed very little after more than 2000 s (Figure 9). If a network is not cross-linked or not tightly entangled, the network should quickly relax, and the relaxation time should be very short. If a network is tightly cross-linked chemically, there should be no relaxation, and the relaxation time should be infinite. While a rubberlike material is held at an initial deformation, which is the relaxation measurement conducting, the stress and relaxation modulus [$G(t)$] will slowly decrease

with time as the cross-linked network approaches an equilibrium condition. The relaxation measurements for the composites soyglyde, milkglyde, and saliglyde showed that they had similar relaxation behaviors as lightly cross-linked rubbers. Overall, the viscoelastic properties studies for these three composites suggested that they have similar viscoelastic properties as some natural and synthetic elastomers, and their viscoelastic behaviors can be controlled by the content of cross-linking. Thus, there should be a high potential to use composites soyglyde, milkglyde, and saliglyde as replacement for some synthetic rubbers.

AUTHOR INFORMATION

Corresponding Author

*Tel: +1-309-681-6341. Fax: +1-309-681-6524. E-mail: Rogers.HarryOkuru@ars.usda.gov.

Notes

Names are necessary to report factually on available data. The U.S. Department of Agriculture neither guarantees nor warrants the standard of the product, and the use of the name by the U.S. Department of Agriculture implies no approval of the product to the exclusion of others that may also be suitable. The authors declare no competing financial interest.

ACKNOWLEDGMENTS

We express gratitude to Karl Vermillion for the NMR spectra and Jason Adkins for technical assistance.

REFERENCES

- (1) Guillet, J. E.; Norrish, R. G. W. Photolysis of poly methyl vinyl ketone formation of Block Polymers. *Nature* **1954**, *173*, 625–627.
- (2) Norrish, R. G. W.; Bamford, C. H. The formation and decay of excited species. *J. Chem. Soc.* **1938**, 1521, 1531–1544.
- (3) Coyle, J. D.; Carless, H. A. J. Photochemical reactions of ferrocenyl ketones. *Chem. Soc. Rev.* **1972**, *1*, 465.
- (4) Wagner, P. J. Type II Photoelimination and Photocyclization of Ketones. *Acc. Chem. Res.* **1971**, *4*, 168.
- (5) Potts, J. E.; Clendinning, R. A.; Ackart, W. B.; Niegisch, W. D. Biodegradation of synthetic polymers containing ester bonds. *Am. Chem. Soc., Polym. Prepr.* **1972**, *13* (2), 629.
- (6) Holmes, P. A. Application of PHB—A Microbially Produced Biodegradable Thermoplastic. *Phys. Technol.* **1985**, *16*, 32–36.
- (7) Leonard, F.; Kulkarni, R. K.; Brandes, G.; Nelson, J.; Cameron, J. J. Synthesis and Degradation of Poly (alkyl α -cyanoacrylates). *J. Appl. Polym. Sci.* **1966**, *10*, 259.
- (8) Allcock, H. R.; Fuller, T. J. The Synthesis and Hydrolysis of Hexa(imidazolyl)-cyclotriphosphazenes. *J. Am. Chem. Soc.* **1981**, *103*, 2250–2256.
- (9) Guillet, J. E.; Heskins, M.; Spencer, L. R. Studies of the biodegradability of photodegraded plastic compositions. *Polym. Mater. Sci. Eng.* **1988**, *58*, 80.
- (10) Vert, M.; Mauduit, J.; Li, S. Biodegradation of PLA/GA polymers: increasing complexity. *Angew. Makromol. Chem.* **1989**, *166/167*, 15.
- (11) Ballard, D. G. H.; Tighe, B. J. Studies of the reactions of the anhydrosulphites of α -hydroxy carboxylic acids. Part II. Polymerisation of glycolic and lactic acid anhydrosulphites. *J. Chem. Soc. B* **1967**, 976–980.
- (12) Kricheldorf, H. R.; Jonte, J. M. Poly(lactic acid)—Degradable plastics. *Coat. Binders Polym. Bull.* **1983**, *9*, 276–283.
- (13) Gilding, D. K.; Reed, A. M. Biodegradable polymers for use in surgery- polyglycolic/poly(acetic acid) homo- and copolymers: 1. *Polymer* **1979**, *20*, 1459–1464.
- (14) Griffin, G. J. L. Biodegradable synthetic resin sheet material containing starch and a fatty material. U.S. Patent 4,016,117, April, 1977.
- (15) Otey, F. H.; Westoff, R. P.; Doan, W. M. Starch-based blown films 2. *Ind. Eng. Chem. Res.* **1987**, *26*, 1659–1663.
- (16) Cornell, H. J.; Maxwell, R. J. Amino acid composition of Gliadin fractions which may be toxic to individuals with coeliac disease. *Clin. Chim. Acta* **1982**, *123*, 311–319.
- (17) Howdle, P. D.; Ciclitira, P. J.; Simpson, F. G.; Losowsky, M. S. Are all gliadins toxic in coeliac disease? An in vitro study of alpha, beta, gamma and w gliadins. *Scand. J. Gastroenterol.* **1984**, *19*, 41–47.
- (18) Hudson, D. A.; Purdham, D. R.; Cornell, H. J.; Rolles, C. J. Non-specific cytotoxicity of wheat gliadin components towards cultured human cells. *Lancet* **1976**, *1*, 339–341.
- (19) Jos, J.; Charbonnier, L.; Mosse, J. The toxic fraction of gliadin digests in Coeliac Disease. Isolation by chromatography on Biogel P-10. *Clin. Chim. Acta* **1982**, *119*, 263–274.
- (20) Van de Kamer, J. H.; Weijers, H. A. Coeliac disease: Some experiments on the cause of the harmful effects of wheat gliadin. *Acta Paediatrica.* **1955**, *44*, 465–469.
- (21) Cornell, H.; Weiser, H.; Belitz, H.-D. Characterization of the gliadin-derived peptides which are biologically active in coeliac disease. *Clin. Chim. Acta* **1992**, *213*, 37–50.
- (22) Xu, J.; Liu, Z.; Erhan, S. Z.; Carriere, C. J. A Potential Biodegradable Rubber—Viscoelastic Properties of a Soybean Oil-Based composite. *J. Am. Oil Chem. Soc.* **2002**, *9*, 593–596.
- (23) Harry-O'kuru, R. E.; Carriere, C. J. Synthesis, Rheological Characterization and Constitutive Modeling of Polyhydroxy Triglycerides of Milkweed Oil. *J. Agric. Food Chem.* **2002**, *50*, 3214–3221.
- (24) Ayorinde, F. O.; Butler, B. D.; Clayton, M. T. Vernonia galamensis: A rich source of epoxy acids. *J. Am. Oil Chem. Soc.* **1990**, *67*, 844–845.
- (25) Ngai, K. L.; Plazek, D. J. Temperature Dependences of the Viscoelastic Response of Polymer System. In *Physical Properties of Polymers Handbook*; Mark, J. E., Eds.; American Institute of Physics: Woodbury, NY, 1966; pp 341–362.
- (26) Ferry, J. D. *Viscoelastic Properties of Polymers*, 3rd ed.; Wiley: New York, 1980.
- (27) Brostow, W.; Kubat, J.; Kubat, M. M. Mechanical Properties. In *Physical Properties of Polymers Handbook*; Mark, J. E., Ed.; American Institute of Physics: Woodbury, NY, 1996; pp 313–334.